Seasonal Variations of MERIS-derived Chlorophyll-a Concentration in the Coastal Waters of Côte d'Ivoire in Relation to Sea Surface Temperature and Hydrography

J.M. Kouadio, F. Mélin, E.V. Djagoua, K. Affian, N. Hoepffner, J.-B. Kassi

Abstract— Remote sensing data from MERIS are used to study the seasonal variations of the chlorophyll-a concentration (Chl*a*) in the coastal region of the Côte d'Ivoire. A ten-year monthly climatology of Chl*a* is described for the Ivorian coastal and offshore domain and analyzed with a similar climatology of sea surface temperature (SST) from the MODIS-Terra mission. The period of highest Chl*a* values extends from June to October with a peak in August-September in association with the minimum values of SST occurring in the upwelling season. Spatially, the highest Chl*a* values appear along the coast. Then the seasonal variations of Chl*a* and SST in the coastal region are specifically analyzed at locations associated with hydrographic measurement stations at the mouth of four major Ivorian rivers. For the four rivers, the maximum of the flow is in September-October, slightly later than the SST minimum. This flow maximum is also close to the Chl*a* peak for three of the rivers. Assuming a simple linear model, 64% to 81% of the variance in Chl*a* can be explained by river flow and SST, with the realtive importance of these two predictor variables varying between rivers. These results highlight the complexity of the Chl*a* variations in these coastal regions and the usefulness of remote sensing techniques for understanding the local ecosystems.

Index Terms— Chlorophyll-a, Côte d'Ivoire, Gulf of Guinea, Remote sensing, Sea surface temperature.

1 Introduction

With a large part of the Earth's population and economic activities concentrated near the sea, coastal ecosystems are under increasing pressure of anthropogenic origin (e.g., [1]), including increased population and economic development, urbanization, waste water discharge and other localized pollution, habitat degradation, or fishing. While being a very productive ecosystem with a rich biodiversity, the Large Marine Ecosystem (LME) of the Gulf of Guinea has a fairly dense coastal population [2] and is clearly subject to these pressures [3], [4]. In that context, it is essential to implement appropriate monitoring strategies. Remote sensing has a role to play as a powerful monitoring tool and for developing a deeper understanding of ecological dynamics. Particularly ocean colour data have been regularly used in assessments of coastal ecosystems (e.g., [5], [6], [7], [8], [9]).

This study contributes to this effort by analyzing the variations of the chlorophyll-a concentration (Chl*a*) in the coastal region of the Côte d'Ivoire (Ivory Coast) which is part of the Gulf of Guinea. Chl*a* is taken as a proxy for phytoplankton abundance that constitutes the base of the marine food chain and is a quantity included in marine ecosystem monitoring programs. The variability of Chl*a* is discussed with respect to distributions of sea surface temperature (SST) for the entire region as well as hydrographic data for the coastal zone. These quantities are relevant for phytoplankton variations since they can be related to nutrient availability that conditions algal growth. One source of nutrients in the region is the upwelling of deep, nutrient-rich, waters that are characterized by lower temperatures [10], [11]. A similar analysis has been presented in [12] at the scale of the Gulf of Guinea using imagery from the Sea-viewing Wide Field-of-View Sensor (SeaWiFS, [13]). The current work focuses on the Ivorian region and relies on a more recent sensor, the Medium Resolution Imaging Spectrometer (MERIS, [14]), from which products are derived on a finer grid (approximately 2-km grid size) that is more suitable for assessing coastal distributions. Furthermore, the analysis is completed by comparing satellite Chl*a* values with hydrographic field data of river flow that is another source of nutrients.

The area of study, data and methods are first introduced. Then the annual cycle of Chl*a* and SST over the Ivorian domain is described and the relationship between Chl*a* and river flow in the coastal zone is discussed.

2 Material and Methods

The Ivorian coast is part of the great ecosystem of the Gulf of Guinea that extends from Guinea Bissau to Angola. It is bounded by the Cape Palmas on the West and by the border with Ghana in the East, with an extent of about 520 km along a thin continental shelf (Fig. 1). The Ivorian coast is fed by a vast river system characterized by two types of rivers. The first is constituted of four main rivers, which take their source in

- *J.M. Kouadio, E.V. Djagoua, K. Affian, and J.-B. Kassi are with the Centre Universitaire de Recherche et d'Application en Télédétection (CURAT) in Felix Houphouet Boigny University, Box 801 Abidjan 22 (Cocody-Abidjan, Côte d'Ivoire), E-mail: vdjagoua@yahoo.fr*
- *F. Mélin and N. Hoepffner are with the E.C. Joint Research Centre, Institute of Environment and Sustainability, 21027 Ispra (Italy).*

zones of savanna further north (Fig. 1). They are, from west to east, the rivers Cavally, Sassandra, Bandama and Comoé. The second group includes local or coastal rivers possibly connected with coastal lagoons (e.g., [15]).

2.1 Chlorophyll-a Concentration Data

The chlorophyll-a concentration (Chl*a*) was derived from the Medium Resolution Imaging Spectrometer (MERIS) on-board the ENVISAT platform that was launched in March 2002 [14]. The MERIS level-1b data (top-of-atmosphere, TOA, radiance) were obtained after the 3rd reprocessing [16] that among other things revised the sensor calibration history, and were processed with the SeaWiFS Data Analysis System (SeaDAS 6.3, [17]) from the TOA data.

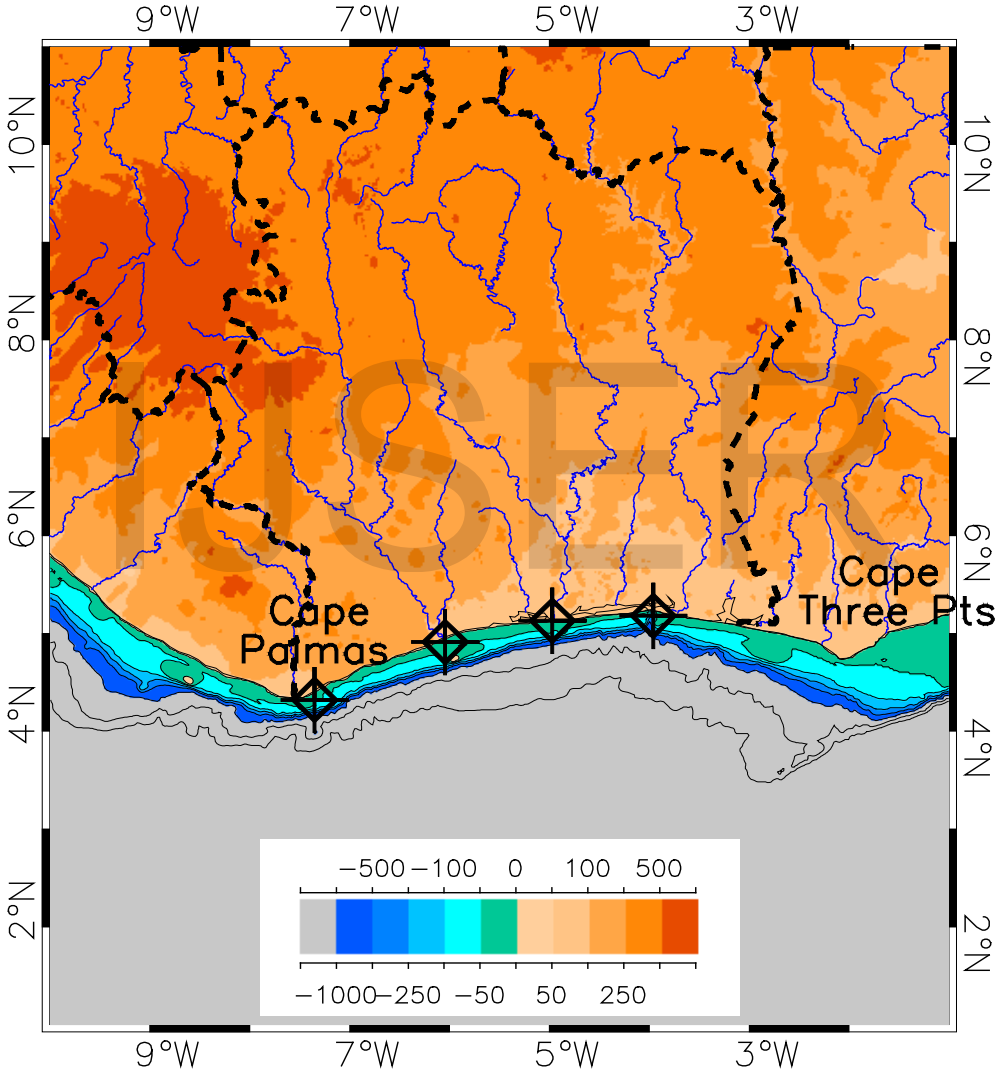

Figure 1: Location of the study area (coastal region of Côte d'Ivoire). Warm colors (orange-red) are for continental regions. The dashed black lines indicate political borders, and blue lines are rivers. The five green-to-blue colors show different depth levels, to 50, 100, 250, 500 and 1000 m.Grey shows waters deeper than 1000 m, with two additional isobaths at 2000 and 3000 m. The four crossed diamonds show the location of hydrographic sampling sites at the mouths of the rivers Cavally, Sassandra, Bandama, and Comoé (from west to east). The Cavally in its southern part follows the border between Côte d'Ivoire and Liberia.

The remote sensing reflectance R_{RS} was derived through the SeaDAS atmospheric correction originally devised by Gordon and Wang [18] and regularly updated (e.g., [19]). Its application to MERIS data, including a process of vicarious calibration, was introduced in [20].

From the spectral values of R_{RS}, Chl*a* is calculated with the MERIS version of the OC4 algorithm [21], OC4E, that relates Chl*a* to the maximum band ratio (MBR) between reflectance values at short wavelengths and a reflectance value in the green (560 nm) through the equations:

$$Chla = 10^{CR} \quad (1)$$

$$CR = 0.3255 - 2.7677R + 2.4409R^2 - 1.1288R^3 - 0.4990R^4 \quad (2)$$

where $R = \log_{10}((R_{RS}\ 443 > R_{RS}\ 490 > R_{RS}\ 510)/ R_{RS}\ 560)$, and $(R_{RS}\ 443 > R_{RS}\ 490 > R_{RS}\ 510)$ is a shorthand representation meaning that the argument of the logarithm is the maximum of three values.

The final product is remapped onto a 2-km resolution grid covering the domain 2°N-6°N, 9°W-1°W. This processing is applied over the period July 2002 to June 2011 that then serves to compute a monthly climatology.

2.2 Sea Surface Temperature Data

Climatological fields of SST are obtained as binned monthly files (2000-2011) from the US National Aeronautics and Space Administration (NASA) and remapped on the same domain as Chl*a*. The selected product is based on a night-time retrieval of SST using the Moderate Resolution Imaging Spectroradiometer (MODIS, [22]) thermal infrared bands [23].

2.3 Hydrographic Data

Daily flows of the four main rivers of the Côte d'Ivoire were also used to assist in the understanding of the time series in coastal waters.

Flow measurements are obtained from conventional stations. They allow the calculation of flow rates through a univocal relationship between height and flow rate. These data were measured on sections of about 410 km² each and not influenced by the ocean tide. These stations are Taté for Cavally, Soubré for Sassandra, Tiassalé for Bandama and M'basso for Comoé. In practice, the stations are home to a data logger that measure discontinuously water level at different time (6 times per day) and stores the information in a file. Field teams conduct regular spot flow measurements fully describing the hydrological regime (high, medium and low water). The set of coincident values of water level and flow rate serves to create a calibration curve that can be applied to the suite of water level automatic records. These data cover the period from 1999 to 2007. Flow rates were obtained from the hydrological service of the water direction (Ministry of Economic Infrastructure).

From these data, the average monthly flow of the different rivers was computed and then a monthly climatology was derived. This information is of help to assess the impact of discharge in the associated coastal area along the Ivorian continental shelf.

2.4 Spatial and Seasonal Variability of SST and Chla

The analysis focuses on the main characteristics of the annual cycle of the Ivorian coast, and thus relies on a monthly climatology for Chl*a* and SST, whereby a value for a month is the average of all monthly averages found for the years in the considered interval. Working with a monthly climatology has also the advantage of maximizing the spatial variability and reducing noise. To compare with the river flow data, the satellite values were extracted and averaged for squares of 5x5 grid points centered on the location of the hydrographic measurement stations that are located just offshore (Fig. 1). These satellite records were considered if at least 25% of the grid points were associated with valid Chl*a* or SST values.

3 Results

3.1 Seasonal Variability of the Concentration of Chlorophyll-a and Sea Surface Temperature

The average annual cycle of Chl*a* is shown on Fig. 2 and can be compared to the equivalent climatology of SST (Fig. 3). The cycle of SST allows the distinction of four marine seasons along the coast of Côte d'Ivoire. These are the small cold season (SCS) in January-February, the great warm season (GWS) from March to May, the great cold season (GCS) from June to September, and the small warm season (SWS) from November to December.

In January the water temperature is generally close to average (slightly less than 27°C). Cold waters (approximately 25°C) are found all along the coast whereas warmer waters are observed offshore. The waters become slightly warmer in February. This season is characterized by a very low spatial coverage by optical remote sensing and even a 10-year monthly climatology does not provide a complete view of the study region. The annual variations of this coverage are related to variations in the cloud cover associated with the latitudinal movements of the Inter-Tropical Convergence Zone (ITCZ) that displace the precipitation band inland (northward) in boreal summer [24], [25] and to the annual cycle of aerosols (with high aerosol loads in boreal winter, [26], [27]). Chl*a* is fairly low offshore, even though an isolated feature of higher Chl*a* can be observed as south as 4°N in January.

From March to May, SST becomes clearly warmer reaching its seasonal peak exceeding 29°C (in April-May). In March and April colder waters can still be noticed along the coast, particularly eastward of the capes (Palmas and Three Points, see Fig. 1), while in May warm waters reach closer to the coast. In March, Chl*a* is again fairly low in the open ocean with higher values north of 4°N. The spatial coverage becomes complete only for the following months. In April, medium values of Chl*a* (0.5-1 mg m^{-3}) are again observed north of 4°N except for some isolated features found offshore. In May, the area of high Chl*a* is restricted closer to the coast, following the retreat of the relatively cold waters.

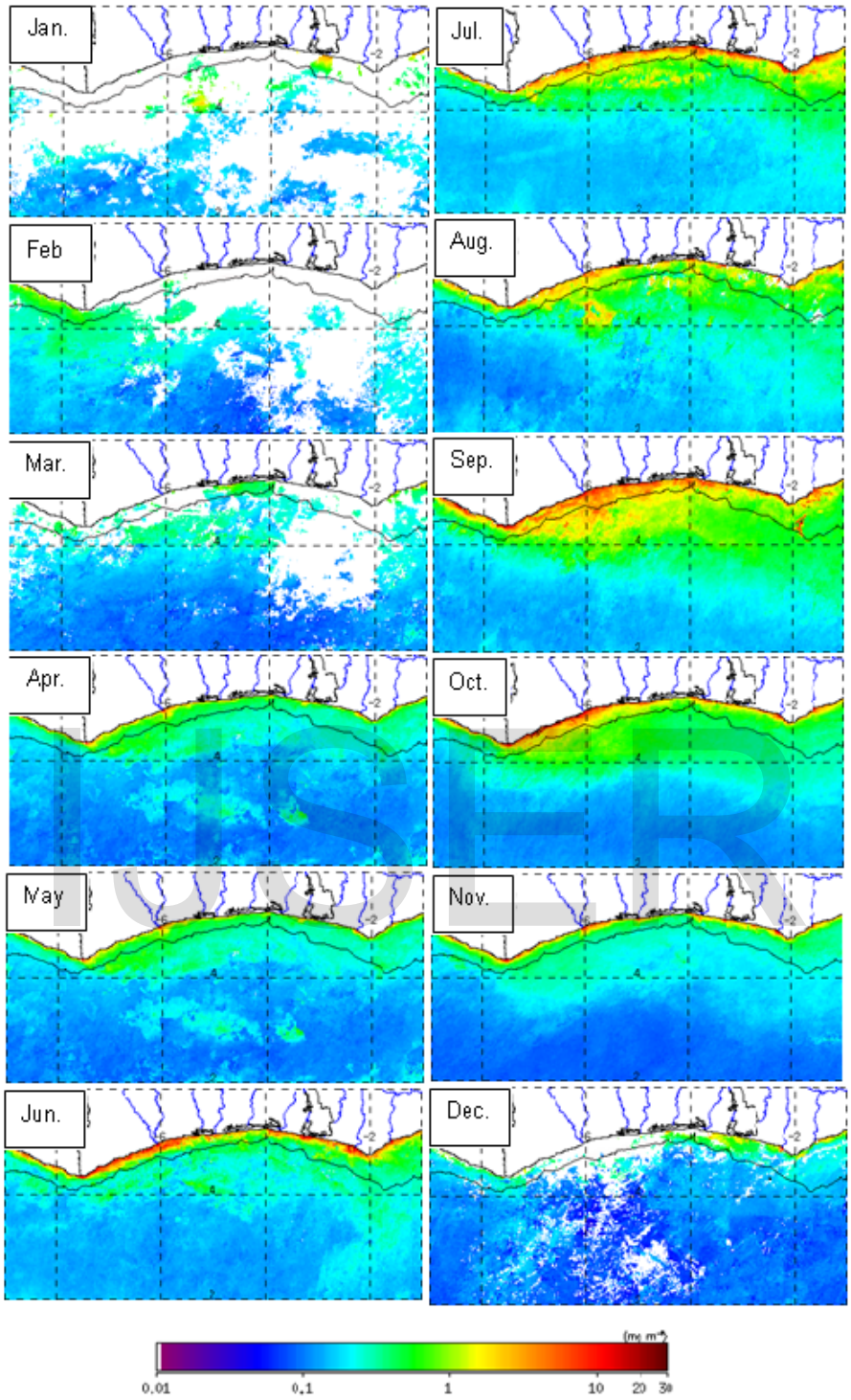

Figure 2: MERIS monthly climatology of chlorophyll-a concentration.

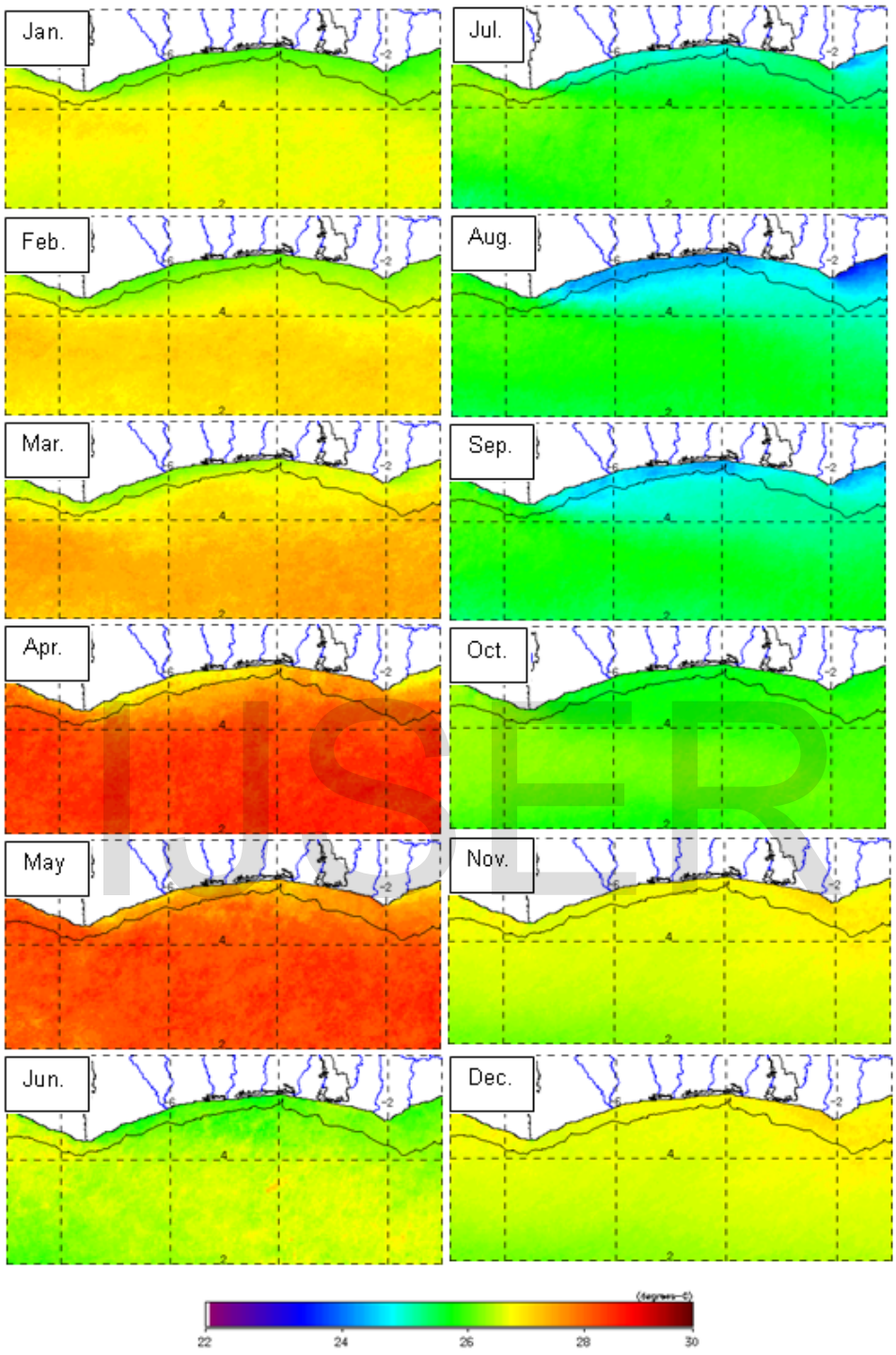

Figure 3: MODIST monthly climatology of sea surface temperature.

In April-May, higher Chl*a* values (approximately 5 mg m^{-3}) can be observed very close to the coast, particularly at the mouths of rivers (e.g., Cavally, Sassandra). Detecting these features fully justify the use of 2-km gridded products for the analysis of coastal variability.

June marks the beginning of the great cold season and shows an abrupt drop in SST over the whole area (less than

27°C). The coldest waters are found along the coast and in the southwest corner. This evolution is associated with an extension offshore of the high Chl*a* band along the coast (>3mg m^{-3}), and a general increase of Chl*a* in the entire open ocean region, particularly in the eastern part. In July the SST has decreased further across the region, and coastal upwelling resulting in minimum SST values is clear in August-September, particularly east of the two capes with temperatures going down to 24°C. In July-August, the Chl*a* values increase in the area (particularly north of 4°N) but it can be noticed that there is not a clear match with the cold SST centres. In September, Chl*a* reaches its annual peak, with the highest values now associated with the coldest SST. The Chla distribution shows values higher than in offshore waters for a large area, limited southward by a line running from the Cape Palmas to the southeast corner of the domain.

The distribution of temperature across the domain is homogeneous in October, with the warm water found offshore now reaching up to the coast. In the subsequent months (Novermber-December), the SST distribution remains homogeneous while increasing. Slightly higher values are found along the 4°N parallel and in the southeastern sector. In October, high Chl*a* values are still found along the coast, while medium values retreat northward to 3.5-4°N. A further decrease takes place in November, and December shows the seasonal low end with small patterns of higher values near the coast and river mouths. However, the spatial coverage for the month of December is again patchy because of atmospheric conditions.

3.2 Seasonal Variability of the Concentration of Chlorophyll-a and Sea Surface Temperature at Selected Coastal Stations

The mean climatological values of the concentration of chlorophyll-a and sea surface temperature during the ten years of the study period have been linked with the flow of several rivers (Fig. 1).

The seasonal variations of the average values of the surface temperature and the concentration of chlorophyll-*a* extracted near the mouth of the Cavally River are shown in Fig. 4. The chlorophyll-a concentration appears fairly low between December and February; however the variations during this season are difficult to characterize as the satellite data coverage is very sparse. This period coincides with the river dry period, from January to March, while the surface temperature is generally high and starts increasing from February onward. After May, the great cold season sets in, with temperature going down to 25°C in August-September. From April to August, Chl*a* is above 1 mg m^{-3}, in association with this cold season and the related upwelling as well as with an increase of the river flow. Chl*a* and river flow are well correlated between June and December with a sharp increase between August and September. It is however noteworthy that Chl*a* decreases before the peak in river flow. This decrease in Chl*a* might be partly due to the end of the upwelling regime as illustrated by the increase in SST from September to November. Similarly, Chl*a* apparently has already increased (April value) before the increase in river flow. It is here relevant to mention that the region (southwestern Côte d'Ivoire) experiences high precipitations in April-June and local, smaller, rivers have a maximum flow in May-June [28], [29].

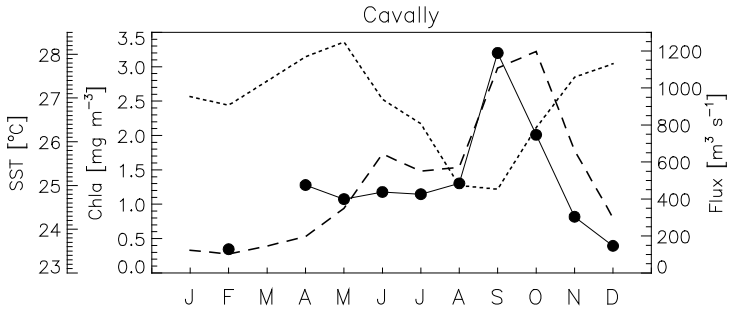

Figure 4: Time series of the chlorophyll-a concentration and sea surface temperature at the mouth of the Cavally River. Chl*a*, SST and river flow are shown by the continuous line with filled circles, dotted line and dashed line, respectively.

Fig. 5 shows the seasonal variations of the SST, Chl*a* and flow for the site associated with the Sassandra River (east of Cavally, Fig. 1).

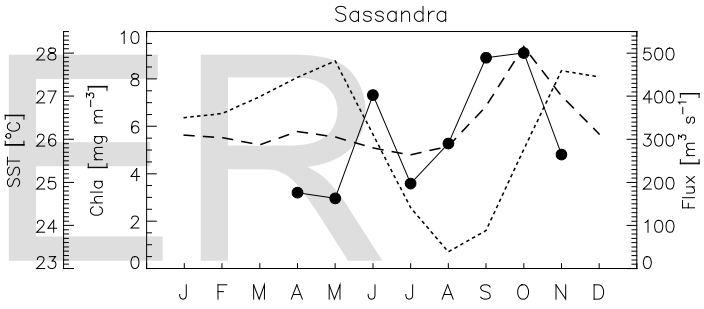

Figure 5: Time series variability of the concentration of chlorophyll and sea surface temperature at the mouth of the Sassandra River. Chl*a*, SST and river flow are shown by the continuous line with filled circles, dotted line and dashed line, respectively.

Again, the full description of the Chl*a* annual cycle is hampered by the lack of coverage in boreal winter. There are common points with the case of the Cavally River, particularly with respect to SST variations, even though the SST minimum is lower (down to 23.3°C). The period of low water is longer, extending from January to August and there is a first Chl*a* peak before the high-flow season (in June) coinciding with the decrease in SST at the beginning of the great cold season. It is worth noticing that, even in the dry season, the flow has significant amplitude (only a factor of 2 difference with respect to the peak, i.e., much less than the factor of ca. 6 seen for the Cavally River) which might be explained by the regulation of the upstream dam. As said for the Cavally River, some local rivers (west of the Sassandra outlet) have a high flow in this period that might have an impact on the Chl*a* series. The major increase in Chl*a* (August-September) corresponds to the minima in SST along the coast (see also Fig. 3) and precedes

the surge in river flow, while the Chl*a* peak (exceeding 9 mg m^{-3}) coincides with the peak in river flow. The Chl*a* maximum is followed by a decrease in November that can be related to both warmer SST and the end of the high-flow season.

As for the other rivers, the flow at the mouth of the Bandama River (Fig. 6) is at a minimum in the first months of the year even though a significant flow amplitude is maintained.

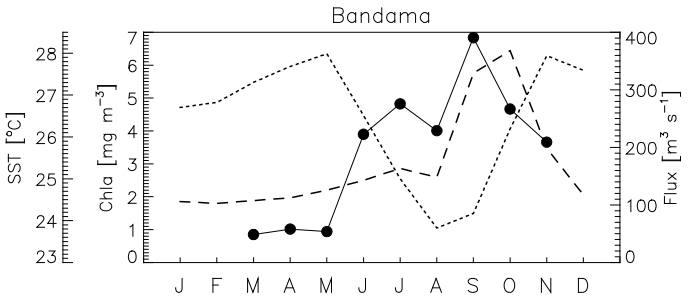

Figure 6: Time series variability of the concentration of chlorophyll and sea surface temperature at the mouth of the Bandama River. Chla, SST and river flow are shown by the continuous line with filled circles, dotted line and dashed line, respectively.

There is a clear minimum in Chl*a* from March to May (below 1 mg m^{-3}), coincident with the great warm season (SST reaches a maximum in May, ~28°C). The Chl*a* values reach higher levels already between June and August while the SST is steadily decreasing. Here again, the coastal region can be influenced by additional inputs from small rivers and lagoons in May-June [15]. Then, Chl*a* increases again in coincidence with the surge in river flow and the main upwelling season to reach its annual peak in September. Finally, Chl*a* decreases before the decline of the high flow while SST is rising again to its second annual peak.

At the Comoé River (Fig. 7), a very low flow rate is measured from December to May, a period with sparse data coverage for Chl*a* and fairly low values (less than 1 mg m^{-3} in March-April), and with increasing SST up to a peak of circa 28°C. After May, Chl*a* increases to reach its annual peak (6 mg m^{-3}) while SST decreases and the river flow slightly increases. In that case, the Chl*a* peak clearly precedes the maximum of upwelling (minimum SST in August-September) and river flow (maximum in September-October), suggesting a significant influence on Chl*a* variations by local flows associated with regional precipitations [30], [31]. The two former factors (upwelling and river discharge) may however contribute to the maintenance of fairly high Chl*a* values until at least September.

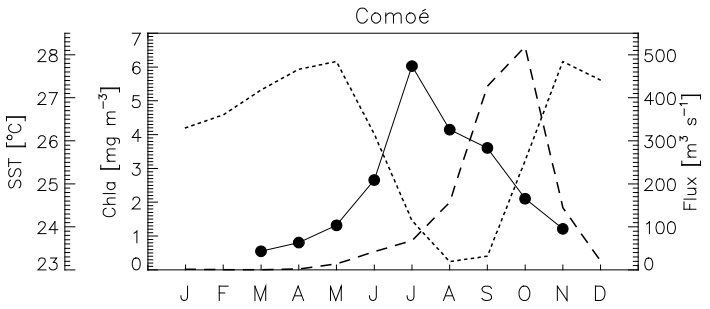

Figure 7: Time series variability of the concentration of chlorophyll and sea surface temperature at the mouth of the Comoé River. Chla, SST and river flow are shown by the continuous line with filled circles, dotted line and dashed line, respectively.

4 Discussion and Conclusion

Satellite data from MERIS were used to document the variations of Chl*a* at the scale of the Ivorian coastal region, and these variations were commented with respect to the variations observed in SST. They show that the period of high Chl*a* broadly extends from June to October with a maximum mostly in August-September coincident with the coldest temperatures associated with upwelling [32]. The observed variations are generally consistent with those described in [12], [33] using SeaWiFS data at the scale of the Gulf of Guinea or for the Ivorian region during the upwelling season. This is an encouraging result in view of creating a long-term data record for the region relying on multiple satellite missions. This being said, some differences are apparent. For instance, Djagoua et al. [33] show Chl*a* values along the coast lower in September than in August, which is opposite to the MERIS annual cycle described here. A dedicated study is needed to understand this type of discrepancies between the climatology of different satellite missions. These discrepancies can originate from actual differences between the data sets associated with each mission and/or from interannual variations (the climatology for each sensor being calculated over different periods).

The description of the annual cycle of Chl*a* and SST at the level of the Ivorian domain has served to put in perspective the analysis made at specific coastal locations for which hydrographic data are available. Phytoplankton in the coastal region can benefit from two main sources of nutrients, the upwelling of cold, nutrient-rich, waters and terrigenous inputs with the former likely being the most important [10]. Locally, it is difficult to assess the relative importance of these inputs in terms of Chl*a* variations since the periods of upwelling and high-flow are actually close in time (shift of 1-2 months between minimum SST and peak flow). The Chl*a* annual peak is well associated with the river maximum for the Canally River, and a second peak in Chl*a* (representing the annual maximum) is also fairly coincident with the high flow for the rivers Sassandra and Bandama. But for these two rivers, there is a first peak in Chl*a* before the increase in river flow, coinciding with the onset of the upwelling season. For these three rivers, the highest rate of increase in Chl*a* (from August to September) corresponds to the annual minimum in SST. For the

Comoé River, the main Chl*a* peak is found earlier at the beginning of the upwelling season (Fig. 7). It is acknowledged that there might be a slight mismatch in the annual cycle of Chl*a* and river flow since the climatology has been computed on different periods (see section 2) and the satellite coverage for the region is irregular due to the atmospheric conditions in the region, but a refined temporal analysis is not possible because the actual monthly hydrographic data are not available. On the other hand the temporal patterns shown by the river flow data can be well trusted since at least the phase of the hydrographic data appears fairly stable between different periods [28]. Finally, the hydrographic data presented do not account for other secondary sources associated with local precipitations or smaller rivers (e.g. [28], [30], [31]).

The general relationship between Chl*a* and river flow is in any case not straightforward. The inputs of rivers also include sediments and dissolved organic matter that increase turbidity and prevent light penetration (e.g., [34], [35], [36]). This effect can therefore introduce a light limitation on phytoplankton growth even in the presence of additional nutrients. The varying concentrations of these optically significant constituents as well as other factors typical of coastal waters like the presence of continental aerosols or possible bottom effects also make the determination of Chl*a* with bio-optical algorithms particularly challenging [37], [38]. The standard band-ratio algorithm used in this study [21] is known to be sensitive to independent variations of non-pigmented particles and chromophoric dissolved organic matter (CDOM) [37], [39], and has shown large uncertainties in coastal waters (e.g., [40]). On the other hand, Djagoua et al. [12] have not detected a significant distribution of turbid waters along the Ivorian coast using a reflectance test [41]. In any case, it is admitted that the Chl*a* values shown on Fig. 4-7 might be affected by significant uncertainties that are hard to quantify in the absence of validation data.

Keeping these cautious notes in mind, a correlation analysis is performed linking Chl*a* with SST and river flow. For the Cavally and Sassandra Rivers, Chl*a* appears more related to the river flow than to SST, with a high correlation coefficient for Cavally (r=+0.80, N=10) and a lower correlation for Sassandra (r=+0.61, N=8), while the correlation of Chl*a* with SST is -0.63 and -0.42 for Cavally and Sassandra, respectively. In the case of the Bandama River, Chl*a* is equally well related to the other two variables (r equal to +0.74 and -0.76 for river flow and SST, respectively; N=9). With its peaks in Chl*a* and river flow clearly shifted, the Comoé River shows a low correlation between Chl*a* and flow (r=+0.21, N=9), whereas the correlation with SST is high (r=-0.85). Performing a multiple linear regression on the Chl*a* values as a function of two explanatory variables (river flow and SST), the correlation coefficient is 0.83, 0.80, 0.90 and 0.88 for the four rivers (west to east), meaning that such as a simple model explains 64% to 81% of the variance in Chl*a*.

As a conclusion, the concentration of chlorophyll-*a* in the Ivorian coastal waters appears greatly related to the input of nutrients from upwelling and from river flows. A simple correlation analysis suggests that most of the Chl*a* variations in coastal waters can be explained by river flow and SST but to a varying extent between rivers. Admittedly the analysis is limited by the uncertainties that likely characterize the standard Chl*a* product used here, and future work should ideally use algorithms more tuned to the type of coastal waters encountered in the Gulf of Guinea, and/or rely on semi-analytical algorithms that compute a full set of optical properties. In that context the collection of field measurements that could serve for the validation of ocean color products in the coastal waters of Côte d'Ivoire would be of great value. Finally, this study stresses the strength of optical remote sensing in monitoring the coastal regions of the Gulf of Guinea and the importance of creating a consistent long-term data record using the past, present and upcoming ocean color missions.

ACKNOWLEDGMENTS

The authors would like to thank the European Commission-Joint Research Centre, Institute for Environment and Sustainability, Ispra, Italy, for this project and their continuous effort in processing images. The contribution of the European Space Agency is also acknowledged, as directly providing MERIS L1A data from 2002 to 2011. NASA is also thanked for the MODIS data.

REFERENCES

[1] H.K. Lotze, H.S. Lenihan, B.J. Bourque, R.H. Bradbury, R.G. Cooke, M.C. May, S.M. Kidwell, M.X. Kirby, C.H. Peterson, and J.B.C. Jackson, J.B.C., "Depletion, degradation, and recovery potential of estuaries and coastal seas," *Science*, vol. 312, pp. 1806-1809, 2006.

[2] C. Small, and R.J. Nicholls, "A global analysis of human settlement in coastal zones," *J. Coastal Res.*, vol. 19, pp. 584-599, 2003.

[3] C.N. Ukwe, C.A. Ibe, B.I. Alo, and K.K. Yumkella, "Achieving a paradigm shift in environmental and living resources management in the Gulf of Guinea: The large marine ecosystem approach," *Marine Pollution Bull.*, vol. 47, pp. 219-225, 2003.

[4] S. Heileman S., "Guinea Current LME," in *The UNEP Large Marine Ecosystems Report – A perspective on changing conditions in LMEs of the world's regional seas*, K. Sherman, G. Hempel (eds), UNEP Regional Seas Report and Studies No 182 United Nations Environment Programme. Nairobi, Kenya, pp. 117-130, 2009.

[5] P.J. Brickley, and A.C. Thomas, "Satellite-measured seasonal and inter-annual chlorophyll variability in the Northeast Pacific and Coastal Gulf of Alaska," *Deep-Sea Research II*, vol. 51, pp. 229-245, 2004.

[6] C. Campillo-Campbell, and A. Gordoa, "Physical and biological variability in the Namibian upwelling system: October 1997–October 2001," *Deep-Sea Research II*, vol. 51, pp. 147-158, 2004.

[7] C. Chen, H. Jiang, and Y. Zhang, "Anthropogenic impact on spring bloom dynamics in the Yangtze River Estuary based on SeaWiFS mission (1998-2010) and MODIS (2003-2010) observations," *Int. J. Remote Sensing*, vol. 34, pp. 5296-5316, 2013.

[8] F. Mélin, V. Vantrepotte, M. Clerici, D. D'Alimonte, G. Zibordi, J.-F. Berthon, and E. Canuti, "Multi-sensor satellite time series of optical properties and chlorophyll-*a* concentration in the Adriatic Sea," *Progress in Oceanography*, vol. 91, pp. 229-244, 2011.

[9] P.J. Werdell, S.W. Bailey, B.A. Franz, L.W. Harding, G.C. Feldman, and C.R. McClain, "Regional and seasonal variability of chlorophyll-a in Chesapeake Bay as observed by SeaWiFS and MODIS-Aqua," *Remote Sens. Environ.*, vol. 113, pp. 1319-1330, 2009.

[10] D. Binet, "Phytoplancton et production primaire des régimes côtiers à upwelling saisonniers dans le golfe de Guinée," Océanogr. Tropicale, vol. 18, no 2, pp. 331-355, 1983.

[11] A. Herbland, and P. Le Loeuff, "Les sels nutritifs au large de la Côte d'Ivoire," in *Environnement et ressources aquatiques de Côte d'Ivoire. 1. Le milieu marin*, Paris, ORSTOM, pp. 123-148, 1993.

[12] E.V. Djagoua, P. Larouche, J.-B. Kassi, K. Affian, and B. Saley, "Variabilité saisonnière et interannuelle de la concentration de la chlorophylle dans la zone côtière du Golfe de Guinée à partir des images SeaWiFS," *Int. J. Remote Sensing*, vol. 32, pp. 3851-3874, 2011.

[13] C.R. McClain, M.L. Cleave, G.C. Feldman, W.W. Gregg, S.B. Hooker and N. Kuring, "Science quality SeaWiFS data for global biosphere research," *Sea Technology*, vol. 39, pp. 10-16, 1998.

[14] M. Rast, J.L. Bezy, and S. Bruzzi, "The ESA Medium Resolution Imaging Spectrometer MERIS - A review of the instrument and its mission," *Int. J. Remote Sensing*, vol. 20, pp. 1681–1702, 1999.

[15] S.K. Konan, A.M. Kouassi, A.A. Adingra, B.K. Dongui, and D. Gnakri, "Variations saisonnières des paramètres abiotiques des eaux d'une lagune tropicale: La lagune de Grand-Lahou, Côte d'Ivoire," *European J. Scientific Res.*, vol. 21, pp. 376-393, 2008.

[16] P. Goryl, J.-P. Huot, S. Delwart, M. Bouvet, E. Kwiatkowska, P. Regner, C. Lerebourg, C. Mazeran, L. Bourg, C. Brockmann, D. Antoine, B. Franz, G. Meister, C. Kent, J. Jackson, K. Barker, S. Lavender, R. Doerffer, J. Fischer, F. Zagolski, G. Zibordi, R. Santer, D. Ramon, J. Dash, and N. Gobron, "MERIS 3rd reprocessing," in *Proc. ESA Living Planet Symposium*, ESA SP-686, (Bergen, Norway, 28 June - 2 July 2010), 2010.

[17] G. Fu, K.S. Baith, and C.R. McClain, "The SeaWiFS Data Analysis System," in *Proc. of the 4th Pacific Ocean Remote Sensing Conference*, (Qingdao, China, July 1998), pp.73-79, 1998.

[18] H.R. Gordon, and M. Wang, "Retrieval of water-leaving radiance and aerosol optical thickness over the oceans with SeaWiFS: A preliminary algorithm," *Applied Optics*, vol. 33, pp. 443-452, 1994.

[19] B.A. Franz, S.W. Bailey, P.J. Werdell, and C.R. McClain, "Sensor-independent approach to the vicarious calibration of satellite ocean color radiometry," *Applied Optics*, vol. 46, pp. 5068-5082, 2007.

[20] F. Mélin, G. Zibordi, J.-F. Berthon, S.W. Bailey, B.A. Franz, K.J. Voss, S. Flora, and M. Grant, "Assessment of MERIS reflectance data as processed with SeaDAS over the European seas," *Optics Express*, vol. 19, pp. 25657-25671, 2011.

[21] J.E. O'Reilly, S. Maritorena, D.A. Siegel, M.C. O'Brien, D.A. Toole, B.G. Mitchell, M. Kahru, F.P. Chavez, P. Strutton, G.F. Cota, S.B. Hooker, C.R. McClain, K.L. Carder, F.E. Mueller-Karger, L. Harding, A. Magnusson, D. Phinney, G.F. Moore, J. Aiken, K.R. Arrigo, R. Letelier, and M. Culver, M., "Ocean color chlorophyll-a algorithms for SeaWiFS, OC2, and OC4: Version 4," *NASA Technical Memorandum 2000-206892*, vol. 11, Chap. 2, pp. 9-23, Hooker, S.B., Firestone, E.R. (Eds.), NASA-GSFC, Greenbelt, Maryland, 2000.

[22] W.E. Esaias, M.R. Abbott, I. Barton, O.B. Brown, J.W. Campbell, K.L. Carder, D.K. Clark, R.H. Evans, F.E. Hoge, H.R. Gordon, W.M. Balch, R. Letelier, and P.J. Minnett, "An overview of MODIS capabilities for ocean science observations," *IEEE Trans. Geoscience and Remote Sens.*, vol. 36, pp. 1250-1265, 1998.

[23] O.B. Brown, and P.J. Minnett, "MODIS Infrared Sea Surface Temperature Algorithm Theorical Basis Document, Ver. 2.0, available at http://modis.gsfc.nasa.gov/data/atbd/atbd/mod25, 1999.

[24] B. Sultan, and S. Janicot, "The West African monsoon dynamics. Part II: The "pre-onset" and "onset" of the summer monsoon," *J. Climate*, vol. 16, pp. 3407-3427, 2003.

[25] G. Gu, and R.F. Adler, "Seasonal evolution and variability associated with the West African monsoon system," *J. Climate*, vol. 17, pp. 3364-3377, 2004.

[26] R.B. Husar, J.M. Prospero, and L.L. Stowe, "Characterization of tropospheric aerosols over the oceans with the NOAA advanced very high resolution radiometer optical thickness operational product," *J. Geophysical Res.*, vol. 102, D14, pp. 16889-16909, 1997.

[27] I. Chiapello, P. Goloub, D. Tanré, J. Herman, O. Torres, and A. Marchand, "Aerosol detection by TOMS and POLDER over oceanic regions," *J. Geophysical Res.*, vol. 105, pp. 7133-714, 2000.

[28] V. Fadika, B.T.A. Goula, F.W. Kouassi, I. Doumouya, K. Koffi, B. Kamagate, I. Savane, and B. Srohourou, "Variabilité interannuelle et saisonnière de l'écoulement de quatre cours d'eau de l'ouest côtier de la Côte d'Ivoire (Tabou, Dodo, Néro et San Pedro) dans un contexte de baisse de la pluviométrie en Afrique de l'Ouest," *European J. Scientific Res.*, vol. 21, pp. 406-418, 2008.

[29] B.T.A. Goula, V. Fadika, and G.E. Soro, "Improved estimation of the mean rainfall and rainfall run-off modeling to a station with high rainfall (Tabou) in southwestern Côte d'Ivoire," *J. Applied Sciences*, vol. 11, pp. 512-519, 2011.

[30] B.T.A. Goula, B. Srohourou, A.B. Brida, B.I. Kanga, K.A. N'Zué, and G. Goroza, "Zoning of rainfall in Côte d'Ivoire," *Int. J. Engineering Science and Technology*, vol. 2, no. 11, pp. 6004-6015, 2010.

[31] Y.K. Kouadio, D.A. Ochou, and J. Servain, "Tropical Atlantic and rainfall variability in Côte d'Ivoire," *Geophysical Res. Lett.*, vol. 30, 8005, 10.1029/2002GL015290, 2003.

[32] R. Arfi, O. Pezennec, S. Cissoko, and M.A. Mensah, "Variations spatiale et temporelle de la résurgence ivoiro-ghanéenne," in *Pêcheries ouest africaines : variabilité, instabilité et changement*, pp. 162-172, Eds. P. Cury, C. Roy, Paris: ORSTOM, 1991.

[33] E.V. Djagoua, J.-B. Kassi, B. Mobio, J.M. Kouadio, C. Dro, K. Affian, and B. Saley, "Ivorian and Ghanaian upwelling comparison: Intensity and impact on phytoplankton biomass," *American J. Scientific and Industrial Res.*, vol. 2, pp. 740-747, 2011.

[34] R.I. Jones, "The influence of humic substances on lacustrine planktonic food chains," *Hydrobiologia*, vol. 229, pp. 73-91, 1992.

[35] D.O. Hessen, and L.J. Tranvik, *Aquatic humic substances: ecology and biogeochemistry*, Berlin: Springer-Verlag, 1998.

[36] F. Gohin, S. Loyer, M. Luven, J.-M. Froidefond, D. Delmas, M. Huret, and A. Herbland, "Satellite–derived parameters for biological modelling in coastal waters: Illustration over the eastern continental shelf of the Bay of Biscay," *Remote Sens. Environ.*, vol. 95, pp. 29-46, 2005.

[37] H.M. Dierssen, "Perspectives on empirical approaches for ocean color remote sensing of chlorophyll in a changing climate," *Proc. U.S. National Academy Sci.*, vol. 107, pp. 17073-17078, 2010.

[38] J.-M. Jaquet, S. Tassan, V. Barale, and L. Sabaji, "Bathymetric and bottom effects on CZCS chlorophyll-like pigment estimation: data from the Kerkennah Shelf (Tunisia)," *Int. J. Remote Sens.*, vol. 20, no. 7, pp. 1343-1362, 1999.

[39] M. Szeto, P.J. Werdell, T.S. Moore, and J.W. Campbell, "Are the world's oceans optically different?," *J. Geophysical Res.*, vol. 116, C00H04, 10.1029/2011JC007230, 2011.

[40] F. Mélin, G. Zibordi, and J.-F. Berthon, "Assessment of satellite ocean color products at a coastal site," *Remote Sens. Environ.*, vol. 110, pp. 192-215, 2007.

[41] S. Ouillon, and A. Petrenko, "Above-water measurements of reflectance and chlorophyll-a algorithms in the Gulf of Lions, NW Medi-

terranean Sea," *Optics Express*, vol. 13, pp. 2531-2548, 2005.